

## [K<sup>+</sup>] Dependence of Open-Channel Conductance in Cloned Inward Rectifier Potassium Channels (IRK1, Kir2.1)

A. N. Lopatin and C. G. Nichols

Department of Cell Biology and Physiology, Washington University School of Medicine, St. Louis, Missouri 63110 USA

**ABSTRACT** Potassium conduction through unblocked inwardly rectifying (IRK1, Kir2.1) potassium channels was measured in inside-out patches from *Xenopus* oocytes, after removal of polyamine-induced strong inward rectification. Unblocked IRK1 channel current–voltage (I–V) relations show very mild inward rectification in symmetrical solutions, are linearized in nonsymmetrical solutions that bring the K<sup>+</sup> reversal potential to extreme negative values, and follow Goldman–Hodgkin–Katz constant field equation at extreme positive  $E_K$ . When intracellular K<sup>+</sup> concentration ( $K_{IN}$ ) was varied, at constant extracellular K<sup>+</sup> concentration ( $K_{OUT}$ ) the conductance at the reversal potential ( $G_{REV}$ ) followed closely the predictions of the Goldman–Hodgkin–Katz constant field equation at low concentrations and saturated sharply at concentrations of >150 mM. Similarly, when  $K_{OUT}$  was varied, at constant  $K_{IN}$ ,  $G_{REV}$  saturated at concentrations of >150 mM. A square-root dependence of conductance on  $K_{OUT}$  is a well-known property of inward rectifier potassium channels and is a property of the open channel. A nonsymmetrical two-site three-barrier model can qualitatively explain both the I–V relations and the [K<sup>+</sup>] dependence of conductance of open IRK1 (Kir2.1) channels.

### INTRODUCTION

Inward, or “anomalous,” rectification of potassium (K) conductance (Katz, 1949) has been described in many cell types, and this phenomenon is characteristic of a whole family of K channels (Kir channels) that differ functionally and, it is now realized, structurally from normal, or outward, rectifying Kv channels (Nichols, 1993). The defining property of strong inward rectifier Kir channels is that conductance falls to essentially zero at membrane potentials that are much positive to the reversal potential for K<sup>+</sup> ions ( $E_K$ ) and increases sharply at negative potentials. In the late 1980s it was shown that internal Mg<sup>2+</sup> ions, driven into the channel by membrane depolarization, block these channels in a voltage-dependent manner, thus reducing macroscopic outward current and producing what is phenomenologically called “inward rectification” (Vandenberg, 1987; Matsuda et al., 1987). However, even in the absence of Mg<sup>2+</sup>, these channels still rectify strongly in a time-dependent manner, and this property has been termed “intrinsic” rectification. The recent availability of cloned strong inward rectifier K channels (Kubo et al., 1993a; Makhina et al., 1994) has led to the recognition that “intrinsic” rectification also results from a voltage-dependent block by internal cationic polyamines—spermine, spermidine, putrescine (Lopatin et al., 1994; Ficker et al., 1994; Fakler et al., 1995; Lopatin et al., 1995)—in further confirmation of Armstrong’s (1969) original suggestion that inward rectification might be caused by cytoplasmic cationic blocking particles.

The inward current through strong inward rectifier channels depends strongly on external [K<sup>+</sup>] ( $K_{OUT}$ ); empirical descriptions of conductance suggest that inward conductance is roughly proportional to the square root of  $K_{OUT}$  (Hagiwara and Takahashi, 1974; Sakmann and Trube, 1984; Kubo et al., 1993a; Makhina et al., 1994; Perier et al., 1994). However, inasmuch as such measurements are likely to be confounded by polyamine- and Mg<sup>2+</sup>-induced rectification, biophysical interpretation of this phenomenon has been limited by studying only inward currents at potentials negative to  $E_K$ . High-level expression of cloned Kir channels in *Xenopus* oocytes, combined with awareness of, and the ability to remove, polyamine-induced rectification, permits examination of the currents through unblocked strong inward rectifier channels over a wide range of potentials. In the present study we have examined currents in the absence of both Mg<sup>2+</sup> ions and polyamines and with full control of extracellular and intracellular K<sup>+</sup> solutions. We report that the conductance of unblocked IRK1 channels saturates sharply when either  $K_{IN}$  or  $K_{OUT}$  is elevated above that on the opposite side of the membrane. I–V relationships are linearized when  $K_{IN} \gg K_{OUT}$  and follow the Goldman–Hodgkin–Katz (GHK) equation when  $K_{OUT} \ll K_{IN}$ , demonstrating internal asymmetry of the ion conduction pathway. Additionally, we show that a square-root dependence of conductance on  $K_{OUT}$  is a property of the open-channel pore (Ciani et al., 1978; Sakmann and Trube, 1984).

### MATERIALS AND METHODS

#### Oocyte expression of Kir channels

cDNAs were propagated in the transcription-competent vector pBluescript SK(–) in *E. coli* TG1. We transcribed capped cRNAs in vitro from linearized cDNAs, using T7 RNA polymerase. Stage V–VI oocytes were isolated

Received for publication 7 September 1995 and in final form 14 May 1996.

Address reprint requests to Dr. Colin G. Nichols, Department of Cell Biology, Washington University School of Medicine, 660 South Euclid Avenue, Box 8228, St. Louis, MO 63110. Tel.: 314-362-6630; Fax: 314-362-7463; E-mail: cnichols@cellbio.wustl.edu.

© 1996 by the Biophysical Society

0006-3495/96/08/682/13 \$2.00

by partial ovariectomy of adult female *Xenopus* under tricaine anesthesia. Oocytes were defolliculated by treatment with 1 mg/ml collagenase (Sigma Type 1A, Sigma Chemical, St. Louis MO) in zero Ca<sup>2+</sup> ND96 (below) for 1 h. 2–24 h after defolliculation, oocytes were pressure injected with ~50 nl of 1–100 ng/ml cRNA. Oocytes were kept in ND96 + 1.8 mM Ca<sup>2+</sup> (below), supplemented with penicillin (100 U/ml) and streptomycin (100 µg/ml) for 1–7 days before experimentation.

## Electrophysiology

Oocytes were placed in hypertonic solution (HY solution, below) to shrink the oocyte membrane from the vitelline membrane. We removed the vitelline membrane from the oocyte, using Dumont #5 forceps. Oocyte membranes were patch clamped with an Axopatch 1D patch clamp apparatus (Axon Instruments Inc., Foster City, CA). Fire-polished micropipettes were pulled from thin-walled glass (WPI Inc., New Haven, CT) on a horizontal puller (Sutter Instrument Co., Novato, CA). Electrode resistance was typically 0.5–2 MΩ when filled with K-INT solution (below), with tip diameters of 2–20 µm. Pipette capacitance was minimized by coating with a mixture of Parafilm (American National Can Co., Greenwich, CT) and mineral oil. Experiments were performed at room temperature in a chamber mounted on the stage of an inverted microscope (Nikon Diaphot, Nikon Inc., Garden City, NY). PClamp software and a Labmaster TL125 digital-to-analog converter were used to generate voltage pulses. Data were normally filtered at 5 kHz, digitized at 22 kHz (Neurocorder, Neurodata, New York, NY), and stored on video tape. Data could then be redigitized into a microcomputer by Axotape (Axon Instruments, Inc.). Alternatively, signals were digitized on line with PClamp software and stored on disk for off-line analysis. In most cases, especially with inside-out patches and low concentration of polyamines or Mg<sup>2+</sup>, leak current and capacity transients were corrected off line with a P/I procedure (+50 mV or higher conditional prepulse). Currents were corrected for rundown wherever possible and necessary.

## Solutions

ND96 solution contained (in mM): NaCl 96, KCl 2, MgCl<sub>2</sub> 1, HEPES 5, pH 7.5 (with NaOH). Hypertonic (HY) solution contained (in mM): KCl 60, EGTA 10, HEPES 40, sucrose 250, MgCl<sub>2</sub> 8; pH 7.0. In most experiments, the control bath and pipette solutions were standard high [K<sup>+</sup>] extracellular solution (K-INT) containing (in mM): KCl 140, HEPES 10, K-EGTA 1, pH 7.35 (with KOH). The bath solution additionally typically contained 1 mM K-EDTA. Concentrations of K<sup>+</sup> up to 20 mM were obtained by dilution of a control K-INT solution with water, with HEPES, EGTA, and EDTA concentrations held constant. High K<sup>+</sup> concentrations were obtained by addition of appropriate amounts of KCl. The pH of all solutions was readjusted to 7.3–7.35. No corrections for osmolarity or ionic strength were made.

## Analysis

Instantaneous I-V relations were obtained by extrapolation of a single exponential function, fitted to the current record, to the beginning of the test pulse, with the steady-state level taken as a free parameter. After washout of polyamines from inside-out patches, currents decay in a single exponential manner with time constants ranging from several milliseconds to seconds (at +80 mV), far slower than capacitive currents. This mono-exponential decay of the current is probably due to the presence of trace amounts of the most potent polyamine, spermine, because with subsequent application of putrescine, spermidine, and spermine the effect of putrescine and spermidine can be washed out within seconds, whereas times up to several minutes are required for removal of the spermine effect. We calculated slope conductance at the reversal potential ( $G_{REV}$ ) from currents in response to voltage ramps with Microsoft Excel Line Estimation Function, using parts of the currents as indicated, for example, by the bold lines in Fig. 2 B below.

The GHK constant field equation 1 (Goldman, 1943) was used to permit quantitative comparison of experimental and theoretical currents:

$$I_{GHK} = AV_M \frac{K_{IN} - K_{OUT} \exp(-\lambda V_M)}{1 - \exp(-\lambda V_M)}, \quad (1)$$

where

$$A \sim \frac{F^2}{RT}, \quad \lambda = \frac{zF}{RT}.$$

One can derive  $G_{REV}$  from  $I_{GHK}$  by taking the derivative at  $V_M = E_K$ , so

$$G_{REV}(K_{IN}, K_{OUT}, V) \big|_{V=E_K} = \frac{d}{dV} \{I_{GHK}(K_{IN}, K_{OUT}, V)\} \big|_{V=E_K}, \quad (2)$$

$$G_{REV} = A \ln \left( \frac{K_{OUT}}{K_{IN}} \right) \left( \frac{K_{OUT} K_{IN}}{K_{OUT} - K_{IN}} \right), \quad (3)$$

where  $G_{REV}$  is a monotonic function of internal [K<sup>+</sup>] ( $K_{IN}$ ) at constant external [K<sup>+</sup>] ( $K_{OUT}$ ) and vice versa. It can also be shown that the slope of the dependence of  $G_{REV}$  on  $K_{IN}$  (at  $K_{IN} = K_{OUT}$ ) is 0.5 in double logarithmic coordinates.

If the electrical field inside the pore is not constant, then a more general form of the GHK equation will be

$$I_{GHK} = AV_M \frac{K_{IN} - K_{OUT} \exp(-\lambda V_M)}{\int_{x=0}^d [1 - \exp(-\gamma f(x)/D(x))] dx}, \quad (4)$$

where  $\tau = F/RT$ ,  $f(x)$  and  $D(x)$  are an arbitrary intramembrane potential and the diffusion coefficient for K<sup>+</sup>, respectively, and  $d$  is the thickness of membrane.  $I_{GHK}$  is still a monotonic function of K<sup>+</sup> concentration. Data are presented as mean  $\pm$  SE wherever possible.

## Perfusion pipette

In some experiments with inside-out patches, the ionic composition in the pipette (outside the membrane) was controlled by use of a pipette perfusion system (Fig. 1A), similar to that used by others (e.g. Tang et al., 1992). This system allows a relatively fast (Fig. 1B) and reversible change of two (control and test) solutions at the tip of the patch pipette. Using this system, we found that success in obtaining a "gigaseal" with giant patches is critically dependent on the geometry of the pipette tip: a conical shape is less effective than a cylindrical one (approximately 10–15 µm in diameter). The length of this cylindrical part of the pipette is a major determinant of the rate of solution exchange. "Positive" pressure (+P) of ~50 cm H<sub>2</sub>O was applied to speed up the application of pipette solutions, while a small negative suction ([-h + (-P)] cm H<sub>2</sub>O) was applied to another line to prevent leakage owing to hydrostatic pressure (-h) and suction (-P) applied to the pipette. The end of the suction tube (ST, Fig. 1A) was placed between the electrode tip and the end of the reference electrode, thus preventing contamination of the solution surrounding the electrode with solution coming from the perfusion tubes (PTs) and stabilizing the electrode potential. Tight sealing of all joints in the system (●) was essential for maintenance of a constant level of pipette solution and hence of stability of the electrode potential.

This perfusion pipette system induces more "equipment" noise at the level of single-channel measurements because of the increased "electrical" size of the pipette. However, with macroscopic currents up to a few nanoamperes, and at low gain, additional noise and capacity currents were practically indistinguishable between perfused pipette and standard holders. After perfusion of a second solution,  $K_{OUT}$  could be calculated from

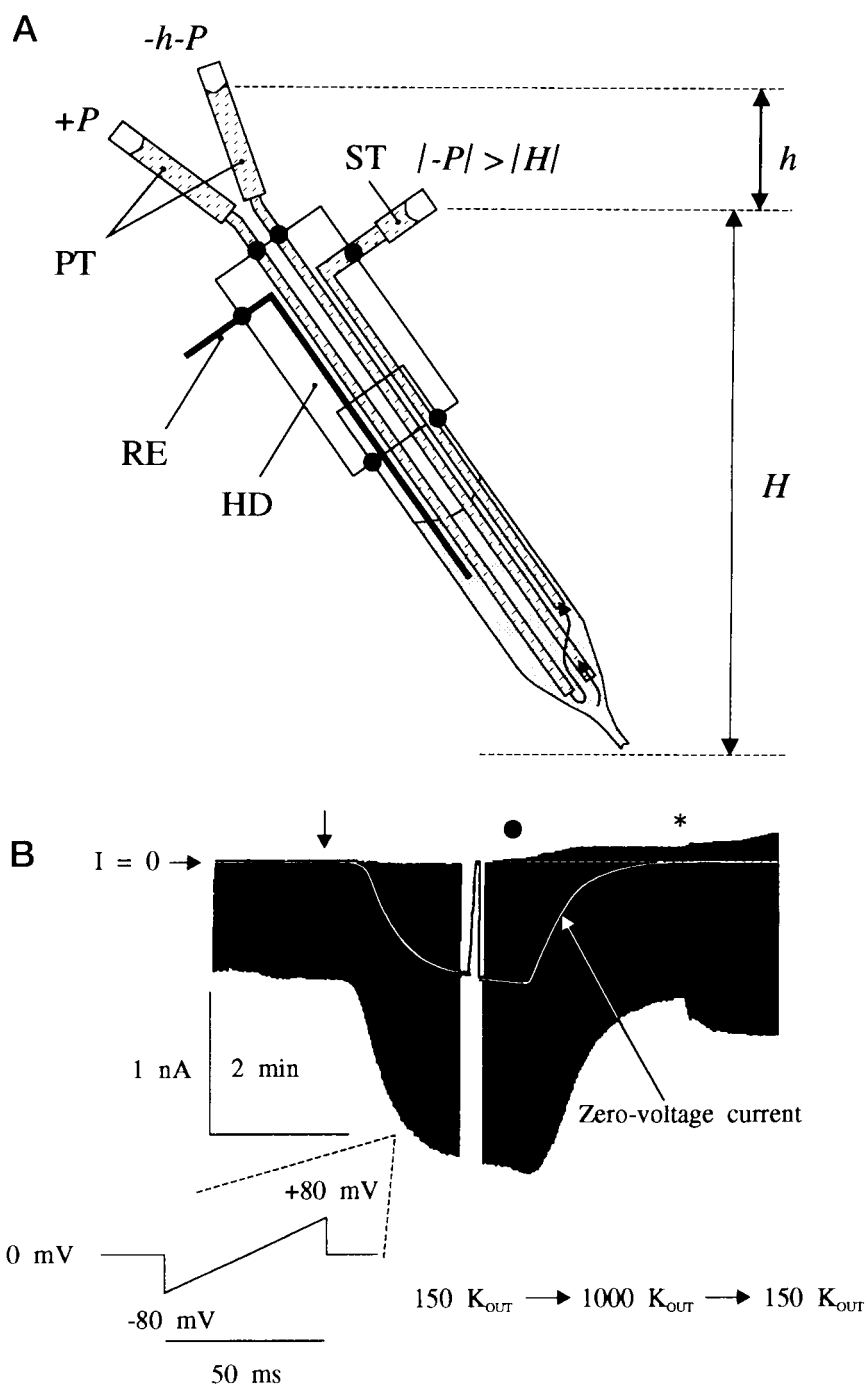


**FIGURE 1** Perfused patch system. (A) Construction of perfusion pipette: HD, pipette holder; ST, suction tube; RE, reference electrode; PTs, perfusion tubes (two);  $+P$ ,  $-P$ , high pressure for perfusion;  $h$ ,  $H$ , solution levels; (●), sealed joints (See Materials and Methods). (B) Characteristic time course of patch perfusion, changing first from 150 to 1000 mM  $K^+$  and then back to 150 mM  $K^+$ . Cell-attached patch currents were measured in response to 50-ms voltage ramps from  $-80$  to  $80$  mV every 1 s. The beginning of patch perfusion is indicated by an arrow, reversal by a ●, and subsequent patch excision by an asterisk. The zero current level is indicated by a white dashed line, and the current at zero membrane potential is highlighted by a white line (manually). At the end of perfusion with 1000 mM, the  $K^+$  reversal potential ( $+43$  mV) was measured in current clamp mode. Some leakage develops at the end of perfusion with 150 mM  $K^+$ .

the reversal potential, assuming that IRK1 channels behave as perfect  $K^+$ -selective electrodes. In most experiments, the calculated steady-state change in  $K_{OUT}$  was approximately 10–20% smaller than expected. This was not due to leakage current because correction assuming leakage causes reversal of current at very positive potentials (current declines owing to residual rectification; see Fig. 2B), which is not reasonable. We attributed the discrepancy in  $K_{OUT}$  to an incomplete change of  $[K^+]$  at the membrane, resulting from a slow component of diffusion. Hence, in such experiments, we have taken the calculated  $K_{OUT}$  as correct. Where this assumption affects the interpretation of the data, this point is considered.

## Modeling

Previous results (Lopatin et al., 1995) showed that there may be multiple binding sites for polyamines, and hence presumably for  $K^+$  ions, inside the pore region of strong inward rectifiers. A two-site three-barrier (2S3B) model (Fig. 6 below) was used for qualitative examination of channel behavior. We followed the approach described by Hille and Schwarz (1978), with some specific modifications. Model parameters were chosen to be asymmetric to accommodate the reasonable suggestions that there is binding at the selectivity filter and that most of the voltage drop occurs at

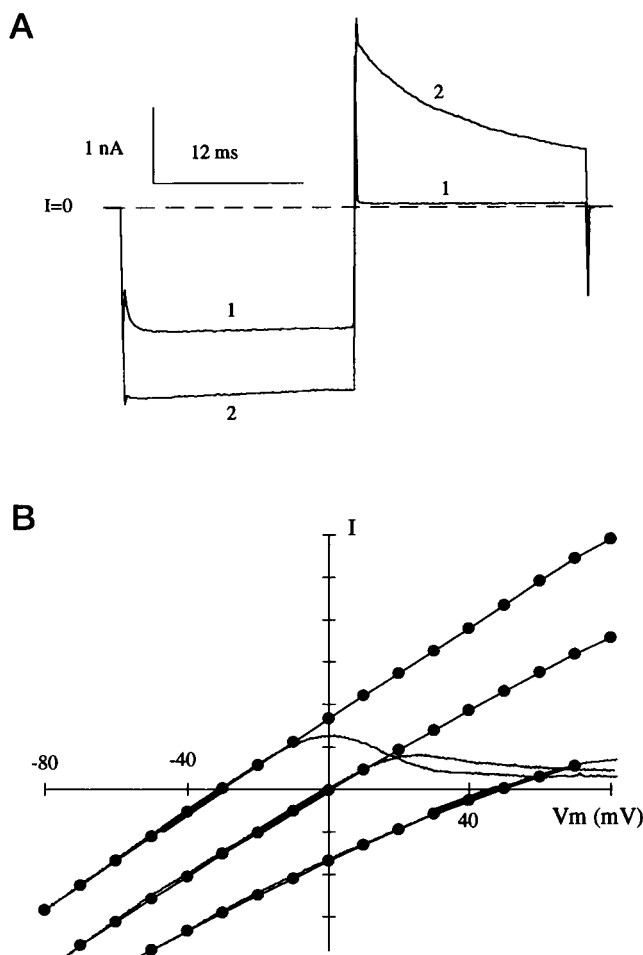


**FIGURE 2** Polyamine-induced rectification. (A) Currents in response to a 25-ms voltage pulse to  $-50$  and then to  $+50$  mV from  $0$ -mV holding potential in a cell-attached patch (1) and in an inside-out patch after washout of polyamines (2). No leak or capacity subtraction was applied. (B) Instantaneous I-V ( $\bullet$ , Inst) relation and I-V relation in response to a 25-ms voltage ramp from  $-80$  mV to  $+80$  mV measured after removal of most of the inward rectification (curve 2 in A). Both I-V relations were normalized to the same value at  $-80$  mV for comparison. The part of the ramp I-V relation highlighted by bold line segments was used for calculation of zero current conductance ( $G_{REV}$ ). Currents are shown with the following  $K_{IN}:K_{OUT}$  ratios (mM)  $500:150$ ,  $150:150$ , and  $25:150$  from left to right.

the intracellular part of the channel, where multiple blocking particles ( $Mg^{2+}$  and polyamines) can bind. Rate constants for jumping into and out of the channel were in the form of  $k = [K]\exp(dG)$  and  $k = \exp(-dG)$ , respectively, where  $[K]$  is the concentration of potassium ions in arbitrary units and  $dG$  is the free-energy difference between the peak and the well for a specific transition normalized to  $RT$  (therefore  $dG$  is dimensionless) in the absence of membrane potential. There is little reason for introducing absolute rate constants (Eyring, 1935); only the relative value of  $G$  is considered. The repulsion factor  $F$  was implemented in a simplified manner (Chizmadjev and Aityan, 1977; Hille and Schwarz, 1978) as an addition ( $\pm F$ ) to  $dG$  for transitions leading into and out of the doubly occupied state. Hence, the full difference in free energy for a specific transition was  $dG + dV \pm F$ , where  $d$  is electrical distance for a specific binding site. The scaling factor for the membrane potential was then set to give the correct reversal potential for potassium ions; potential therefore has real meaning, whereas current and conductance are in arbitrary units.

Microsoft Excel was used to solve the system of linear equations describing the model. The solution was obtained by use of a matrix approach, and corresponding voltage and concentration dependences were automatically displayed with the use of Macro facilities.

## RESULTS

### Kir2.1 currents in the absence of $Mg^{2+}$ or polyamines

To study the K<sup>+</sup> conductance of unblocked IRK1 (Kir2.1) channels, we isolated inside-out patches from *Xenopus* oocytes expressing IRK1 channels at high density into  $Mg^{2+}$ -free solution buffered with EDTA. Macroscopic currents were measured after careful washout of intrinsic rectifying factors (Lopatin et al., 1994) until only a small residual, slow component of rectification at positive membrane potential (up to  $+80$  mV) remained. Under these conditions, residual current decay at positive potentials followed a monoexponential time course (Fig. 2 A), and all patches with  $\tau_{+50} < 25$  ms were discarded from analysis. As shown in Fig. 2 B, currents in response to 25-ms voltage ramps (from  $-80$  to  $+80$  mV) can still display significant inward rectification relative to instantaneous I-V relations, despite intensive washout of polyamines. However, in the range of inward currents, and in the vicinity of the zero current potential, both relationships coincide. This is also true for nonsymmetrical  $[K^+]$  solutions (Fig. 2 B), reflecting the fact that the voltage around which the current rectifies shifts, even under these conditions, almost directly with  $E_K$ . Currents in response to voltage ramps were used to estimate the zero current conductance ( $G_{REV}$ ), but we constructed current-voltage (I-V) relations from instantaneous currents by using step voltage protocols.

### Internal $[K^+]$ dependence of IRK1 conductance

Internal  $[K^+]$  ( $K_{IN}$ ) was varied from 25 to 650 mM while external  $[K^+]$  ( $K_{OUT}$  – pipette) was kept at 150 mM. Substituting  $K^+$  by bigger, nonpermeant cations, such as NMDG<sup>+</sup>, to keep ionic strength at control caused a pronounced fast, and shallow, voltage-dependent block, obviating true measurements of K<sup>+</sup> conductance over the whole range of membrane potentials (cf. Neyton and Miller, 1988). Fig. 3 shows IRK1 currents in response to 25-ms voltage ramps at different  $K_{IN}$  and the corresponding  $G_{REV}$ -V relation.

The  $K_{IN}$  dependence of conductance displays clear saturation at concentrations above 150 mM, whereas it closely follows the predictions of the GHK equation at lower concentrations. When  $K_{IN}$  was changed, experimentally observed reversal potentials differed by a few millivolts (especially at extreme concentrations) from that of a perfectly K<sup>+</sup>-selective channel. This was normally corrected on the assumption that this discrepancy was due to linear leakage currents, although this correction did not qualitatively affect the results.

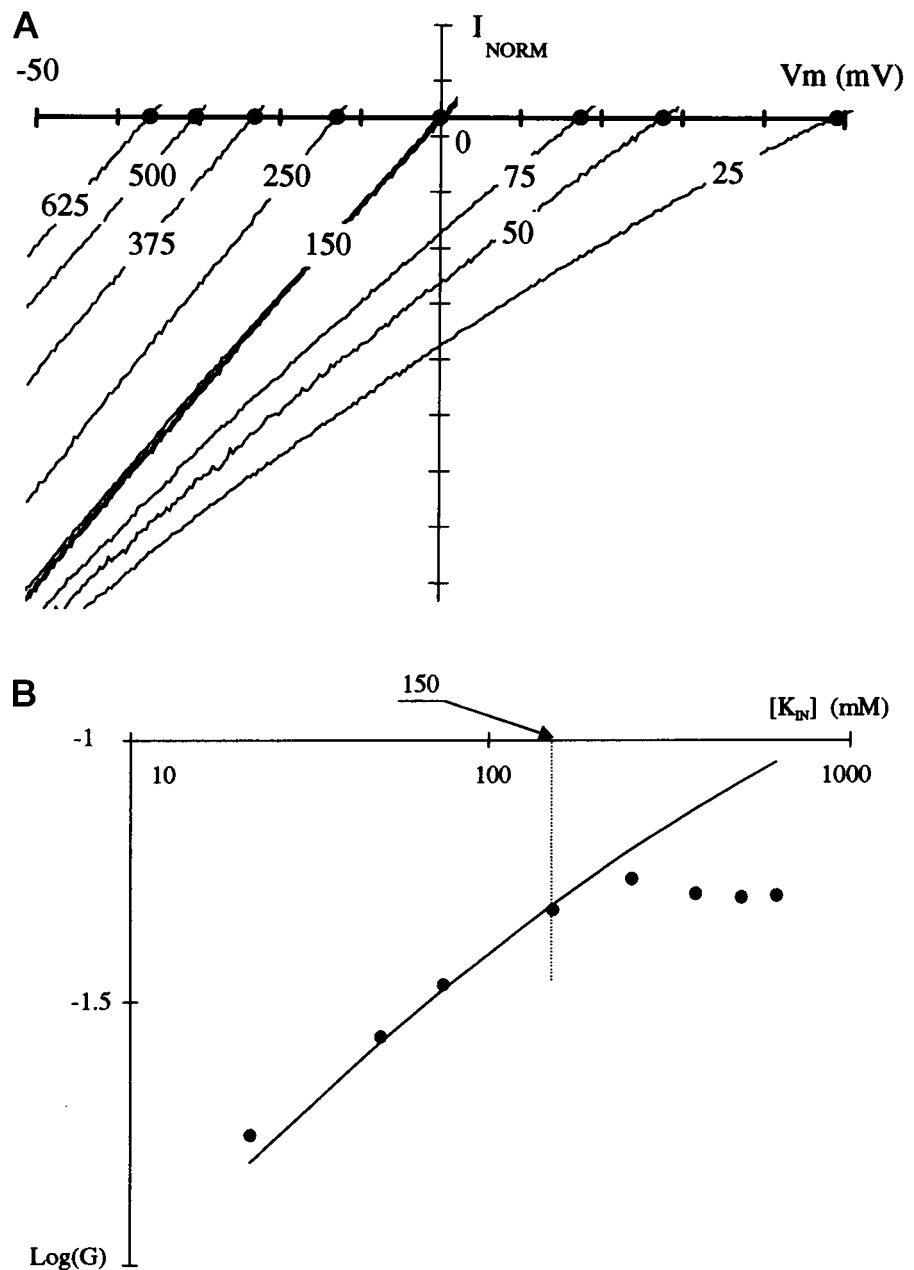


**FIGURE 3** Dependence of IRK1 conductance on  $K_{IN}$ . (A) Current traces in response to voltage ramps (25 ms) from  $-80$  to  $+80$  mV during perfusion with different  $K_{IN}$  (mM): 625, 500, 375, 250, 150, 75, 50, and 25 mM from left to right. Currents are from different patches and are normalized to currents in symmetrical 150-mM  $K_{IN}$  in the same patch (each curve superimposed). (B) Double logarithmic plot of zero current conductance (●,  $G_{REV}$ , arbitrary units) versus  $K_{IN}$ . The solid curve shows the best fit of the GHK equation (Eq. 2) to the points at  $K_{IN}$  less than 150 mM.

### External $[K^+]$ dependence of IRK1 conductance

We measured the external  $[K^+]$  ( $K_{OUT}$ ) dependence of conductance in inside-out patches by varying  $K_{OUT}$  within the experiment, using the pipette perfusion system described in Materials and Methods.  $K_{OUT}$  was varied between 150 and 1000 mM while  $K_{IN}$  was kept at 150 mM. Attempts to use the perfused pipette system to reduce  $K_{OUT}$  below 150 mM failed because of the smaller ionic currents and relatively large leakage that developed during perfusion. Nonperfused patches were stable, with low  $K^+$  concentration in the pipette, and reliable currents could be measured (see below), although direct comparison of conductance at different  $K_{OUT}$  was not then possible. Fig. 4A shows a series

of currents in response to voltage ramps at different times during pipette perfusion with 1000 mM  $K^+$ . Zero current conductance ( $G_{REV}$ ) levels off at concentrations above 150 mM, as seen by comparison with the predictions of the GHK equation (Fig. 3 B). As discussed in Materials and Methods,  $K_{OUT}$  was estimated from the current reversal potential in perfused patches. The calculated steady-state concentration was typically  $\sim 20\%$  less than the perfusing solution, and this difference was attributed to incomplete change of solution at the very tip of the pipette rather than to incorrect estimation of reversal potential as a result of leakage (see Materials and Methods). Nevertheless, even correcting for assumed leakage does not significantly alter

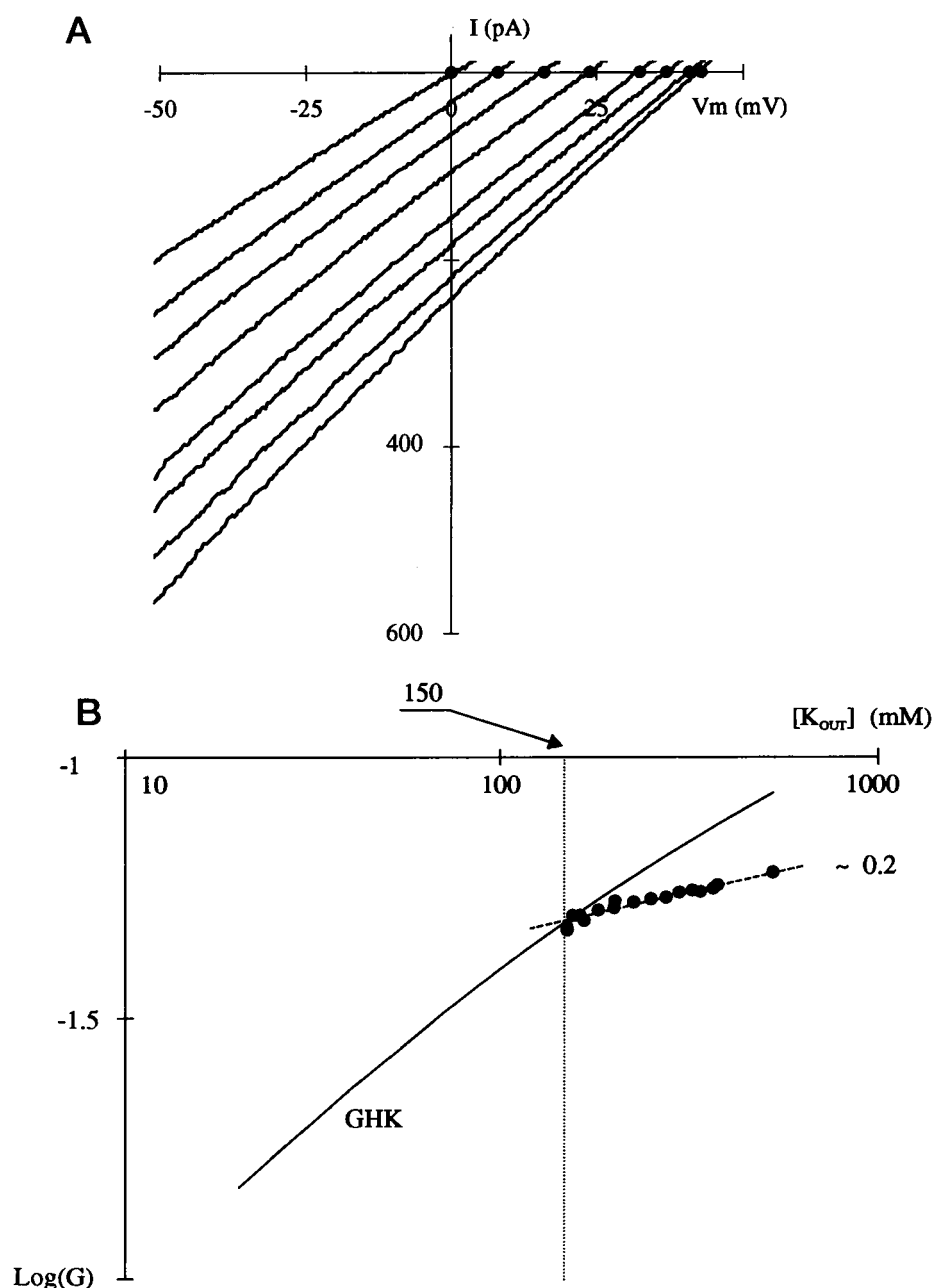


FIGURE 4 Dependence of IRK1 conductance on  $K_{OUT}$ . (A) Family of inside-out current traces in response to voltage ramps (50 ms) from  $-80$  to  $+80$  mV taken at different times during pipette perfusion with 1000 mM  $[K^+]$ . (B) Double logarithmic plot of zero current conductance ( $\bullet$ ,  $G_{REV}$ , arbitrary units) versus  $K_{OUT}$ . The solid curve shows  $G_{REV}$  calculated according to the GHK equation. Linear approximation of the  $G_{REV}$   $K^+$  dependence over this  $[K^+]$  range gives a slope of  $0.20 \pm 0.03$  ( $n = 3$  patches).

the calculated steepness of the dependence of  $G_{REV}$  on  $K_{OUT}$ , which can be approximated by a line with a slope of  $0.2 \pm 0.03$  ( $n = 3$ ; Fig. 4 B).

### Voltage dependence of IRK1 conductance

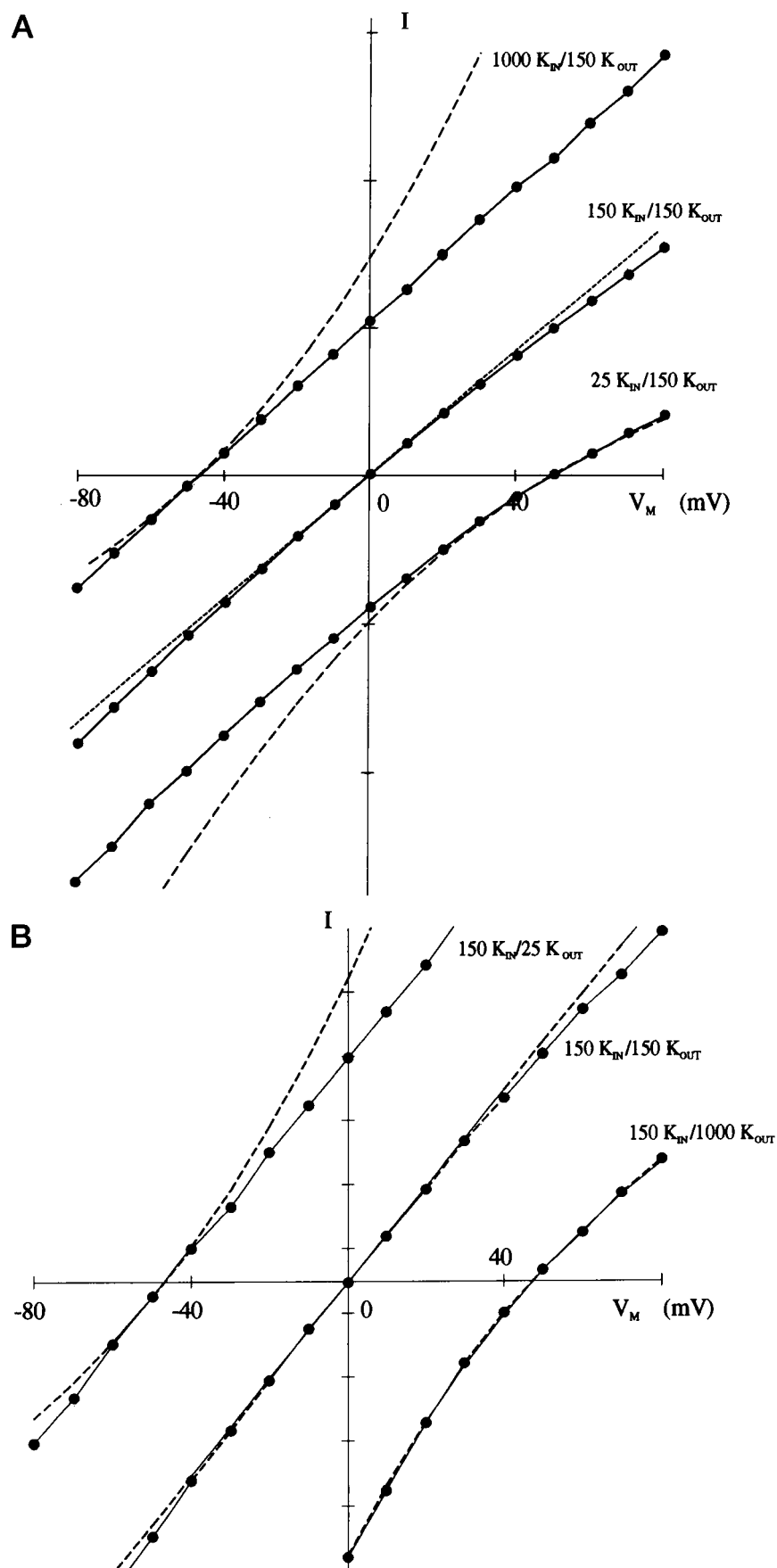
Even with symmetrical potassium solutions (150  $K_{IN}$ :150  $K_{OUT}$ ), I-V curves obtained either in response to voltage ramps (Figs. 2–4) or by calculation of instantaneous relationships (Figs. 2 B and 5) display some inward rectification within the range of potentials from  $-80$  to  $+80$  mV. In contrast, the instantaneous I-V relations do not rectify in conditions that bring  $E_K$  to extreme negative values either by increasing intracellular or by decreasing extracellular

$[K^+]$ . No matter how this negative reversal potential is reached, I-V relations are almost linear (Fig. 5 A and B). In contrast to this, I-V relations obtained in nonsymmetrical  $K^+$  conditions that bring  $E_K$  to extreme positive values are always inwardly rectifying, though not as strongly as predicted by the GHK equation (Eq. 1).

## DISCUSSION

### Multi-ion pore nature of Kir channels

It has been realized for many years that K channels are long pores through which  $K^+$  ions move in single file (Hille and Schwarz, 1978). Several  $K^+$  ions can occupy the channel at



any one time, and there may be a strong electrostatic interaction between ions inside the pore. This realization is based on several characteristic properties of ion conduction through potassium channels, namely, flux coupling (Hodgkin and Keynes, 1955), anomalous mole fraction effect (Hagiwara et al., 1977; Shapiro and DeCoursey, 1991), saturation (Hill et al., 1989; Coronado et al., 1980; Blatz and Magleby, 1984) and decline of conductance at high K<sup>+</sup> concentrations (Wagoner and Oxford, 1987; Villarroel et al., 1988; Lu and MacKinnon, 1994a), all of which contradict simple rules based on independent diffusion of ions inside the pore. Most of this previous research was performed on weakly rectifying or voltage-activated K channels, and until now strong inward rectifiers have essentially not been considered. This has been so because most of the pore properties of strong inward rectifiers are normally overshadowed by the presence of rectification, combined with unavailability of inward rectifier preparations in which ionic conditions on both sides of the membrane could be well controlled. Recent progress in cloning Kir channels (Ho et al., 1993; Kubo et al., 1993a,b) has greatly improved the ability to examine the biophysical properties of inward rectifier channels. The ability to examine macroscopic currents in inside-out patches has led to the discovery that rectification in these channels results primarily from a markedly voltage-dependent block of the channel by intracellular polyamines (Lopatin et al., 1994; Ficker et al., 1994; Fakler et al., 1995; Lopatin et al., 1995) and to the location of the binding sites for these polyamines (Fakler et al., 1994; Yang et al., 1995).

In single-channel measurements it is not feasible to observe the time course of washout of polyamines, and it is therefore difficult to assess the degree of relief of rectification. Macroscopic currents allow us to observe quantitatively the removal of polyamines from inside-out membrane patches and then to examine the properties of the unblocked channel while accounting for the presence of residual polyamines. In this regard, complete washout of exogenously applied spermidine or putrescine occurs within a few seconds, but washout of spermine can take minutes, and it is likely that spermine is the predominant species responsible for residual slow rectification (Fig. 2). Single-channel data might be useful in studying kinetic properties (opening and closing) of these channels, but true intrinsic gating seems to be absent in the absence of rectifying factors such as Mg<sup>2+</sup> and polyamines (Lopatin et al., 1994). (Note: We cannot formally exclude the possibility that the observed shallow instantaneous rectification results from a very fast block by residual polyamines. By use of coated electrodes, the macroscopic capacity transient time constant is reduced to less than 10 microseconds, and residual rectification is still apparently instantaneous. The relatively low single channel conductance of IRK1 channels (~20 pS) means that minimal filtering of ~2 kHz would be necessary to resolve single channels from the noise. Such a fast block as that necessary to cause the inward rectification would then be unresolvable and would be observed only as an apparent reduction of the single-channel current). The results de-

scribed above show that conduction properties of unblocked IRK1 channels are consistent with the idea of strong inward rectifiers being a single file pore.

### K<sup>+</sup> conductance of an unblocked IRK1 channel: a barrier model of ion permeation

If an unblocked ion channel were to obey the constant-field theory (GHK equation, Goldman, 1943; Eq. 1), then the corresponding [K<sup>+</sup>] and voltage dependence of conductance should be observed. The GHK equation assumes that K<sup>+</sup> ions diffuse freely and independently of one another under the influence of a constant electrical field. This means that 1) in symmetrical ionic conditions the I-V relation should be linear and appropriate curvature should be observed in nonsymmetrical conditions and 2) no saturation of conductance should be observed as K<sub>IN</sub> or K<sub>OUT</sub> is increased. The present results show that neither prediction is met in the unblocked IRK1 channel. If it is assumed that the electrical field inside the pore is not constant, then the denominator in the GHK equation (Eq. 4) might, in principle, change the shape of the I-V relation to that seen in a particular experiment. However, overall behavior, including conductance saturation, cannot be reproduced by such an adjustment. Hence, we must discard the idea of ion independence and can suggest instead that ions interact with one another in the IRK1 channel pore and with specific binding sites. This can be modeled by use of a multi-ion barrier model (Hille, 1975; Hille and Schwarz, 1978; Chizmadjev and Aityan, 1977; Hill and Chen, 1971; Schumaker and MacKinnon, 1990; Alvarez et al., 1992). It has been shown that many specific properties of long pores, including saturation (Cecchi et al., 1986; French et al., 1994; Hill et al., 1989; Chang et al., 1994) and even decline of conductance (Finkelstein and Andersen, 1981; Wagoner and Oxford, 1987; Lu and MacKinnon, 1994a) can be adequately described by this approach. The aim of the present modeling is to determine whether a simple 2S3B model (Fig. 6) can qualitatively explain the observed phenomena and to demonstrate whether the general behavior of the model under different conditions corresponds to that observed experimentally. The excessive potential freedom of such barrier models requires consideration of as many experimental data as possible to maximize the usefulness of the exercise. Recent evidence suggests that the pore of strong inward rectifier channels might be long enough to accept more than one spermine molecule (Lopatin et al., 1995; Yang et al., 1995). Although it is not clear how these molecules are actually located or folded inside the pore, their size (~20 Å long and 4 Å in diameter) and charge (+4) suggest that there may be a lot of space within the channel pore when it is approached from the inside. To accommodate this suggestion, as well as other conduction properties described above, the main features of the model are as follows: 1) The pore is not symmetrical (see Results); the central barrier is located closer to the outer part of the channel. 2) The side barriers



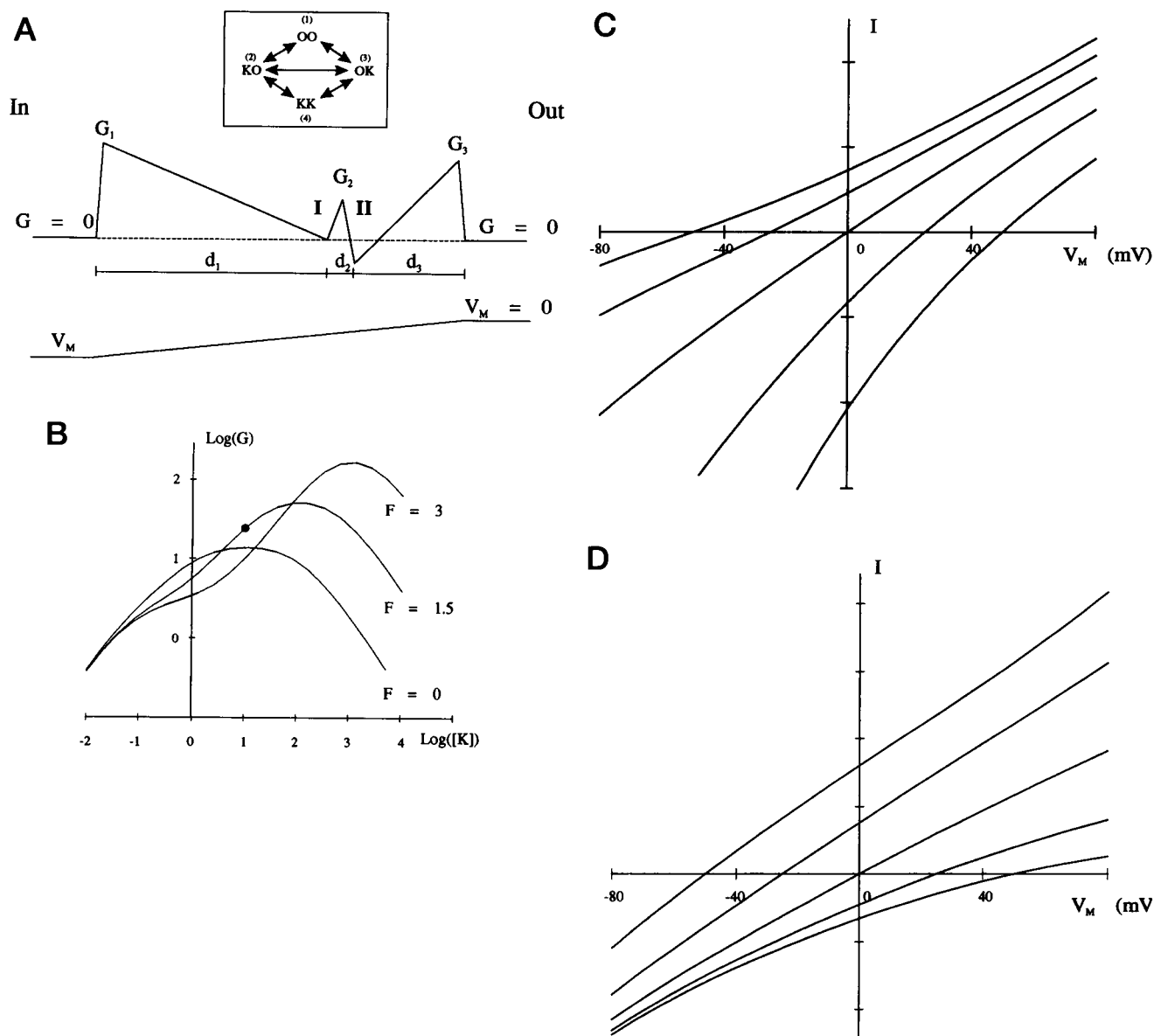


FIGURE 6 2S3B model. (A) Energy profile of the model. Specific parameters were as follows:  $d_1 = 65\%$ ,  $d_3 = 25\%$ , and  $d_2 = 10\%$  (electrical distances for transitions, expressed as % of total membrane potential drop);  $G_1 = 9$ ,  $G_3 = 7$ ,  $G_2 = 2.5$ ,  $G_I = 0$ , and  $G_{II} = -2.5$  (barrier heights and well depths, respectively, dimensionless and defined as the free energies divided by  $RT$ ; see Materials and Methods). (Insert) Possible  $K^+$  transitions according to the scheme in (A). (B)  $[K^+]$  dependence of  $G_{REV}$  for the 2S3B model in (A). Slope conductance at zero membrane potential is plotted against  $\log[K^+]$  for three different repulsion factors,  $F = 0$ ,  $F = 1.5$ , and  $F = 3$ . "Control"  $[K^+] = 10$  (1 in a log scale) and repulsion factor  $F = 1.5$  were chosen for further modeling, as indicated by (●). (C), (D), Families of I-V relations calculated for the 2S3B model in (A), with (C) constant  $K_{IN} = 150$  mM and different  $K_{OUT}$ , giving  $E_K$  in the range of  $\pm 50$  mV and (D) constant  $K_{OUT} = 150$  mM and different  $K_{IN}$ , giving  $E_K$  in the range of  $\pm 50$  mV.

are located close to the inside and the outside, respectively, of the membrane; most of the voltage dependence for binding sites is in the "off" rates (Lopatin et al., 1995). 3) The central barrier is smaller than the side barriers; i.e., the rate-limiting step is entry to (or exit from) the pore (owing to dehydration). 4) The outermost binding site is deeper than the inner binding site and the outermost barrier is smaller than the inside one. Such a profile can also account for the  $K_{OUT}$  dependence of polyamine-induced rectification (unpublished observations), assuming that internal polyamines

permeate the channel up to, but not into, this site. 5) There is electrostatic repulsion between  $K$  ions inside the pore.

Analytical solutions for such a model are not practical, and investigation of the model behavior requires numerical simulations. Fig. 6 B shows the dependence of slope conductance at zero membrane potential ( $G_{REV}$ ) on  $[K^+]$  (symmetrical) with different repulsion factors ( $F$ ). This plot underlines two characteristic properties of long single-file models: 1) saturation and further decline of conductance at high  $[K^+]$  and 2) the fact that electrostatic repulsion spreads

out conductance over a wide range of concentrations (Hille and Schwarz, 1978). It has been pointed out (Hille and Schwarz, 1978) that, because conductance may display multiple flat (descending) and rising stretches (two local peaks for two-site models) it becomes difficult to determine the appropriate range of concentrations where the real channel operates. It appears from the results presented above that IRK1 channels operate close to saturation, so we have modeled the control (150 mM) [K<sup>+</sup>] on the second rise of conductance, with repulsion factor  $F = 1.5$ , close to the final, declining, phase (Fig. 6 B, ●).

Fig. 6 C and D shows that the selected energy profile (Fig. 6 A) can produce I-V relations in different ionic conditions with characteristics similar to those found experimentally. First, because of asymmetry in the energy profile, the I-V relation in symmetrical [K<sup>+</sup>] rectifies inwardly. Second, in nonsymmetrical [K<sup>+</sup>] solutions that bring  $E_K$  to extreme negative values, the I-V relations are linearized. This type of linearization has also been shown theoretically by Hill and Chen (1971) for a 2S3B model. Conversely, I-V relations become convex in solutions that bring  $E_K$  to extreme positive values. In this range of reversal potentials the predicted I-V relations tend to be somewhat more convex than the experimental data and coincide with GHK equation, but the general behavior of the model-predicted I-V relations with different  $K_{IN}$  reproduces that of experiments.

After setting of the "reference" point for conduction in symmetrical solution (Fig. 6 B), the dependence of current on  $K_{IN}$  can be obtained and compared with experiment. Fig. 7A shows that the 2S3B model, with parameters described above, gives a qualitative approximation of the experimental data, although the conductance saturation is shallower, with most deviation from experimental data at high  $K_{IN}$ . The experimentally observed  $G_{REV}$  is predicted by the GHK equation in the range of  $K_{IN}$  concentration lower than 150 mM (Fig. 2), with a slope of 0.5 at  $K_{IN} = K_{OUT}$ . However, when  $K_{IN}$  is increased above  $K_{OUT}$ , channel conductance levels off rather steeply. Although we failed to obtain a full complementary set of data by lowering  $K_{OUT}$  while keeping  $K_{IN} = 150$  mM, we may predict (see Sakmann and Trube, 1984) that in this case  $G_{REV}$  will also follow close to the GHK predictions with a slope close to 0.5 while saturating steeply at  $K_{OUT} \geq K_{IN}$ , as observed experimentally (Fig. 4).

Fig. 7 shows that the shape of the concentration dependence of conductance in nonsymmetrical solutions is extremely sensitive to the position of the side energy peaks (and wells, not shown) whereas in symmetrical solutions the shape is independent of the side energy peak positions. When side peaks (or wells or both) are moved from deep inside the pore to the edge of the voltage field,  $G_{REV}$  in nonsymmetrical solutions changes dramatically, approaching the GHK prediction and hence the experimentally observed  $G_{REV}$  at low  $K_{IN}$  and then leveling off and declining sharply at  $K_{IN} \geq K_{OUT}$ . In our experiments we did not reach high enough concentrations to see a real decline in conductance, so it remains to be established whether such a decline

really does exist and, if so, at what concentrations. In the model, it was not possible to have a very steep  $G_{REV} - K_{IN}$  dependence while keeping I-V relations linearized at negative  $E_K$ .

### Comparison with previous studies

Although earlier examinations of the [K<sup>+</sup>] dependence of inward rectifier conductance were made without knowledge of the mechanism of steep inward rectification, it is likely that polyamine-induced rectification was at least partially removed in studies using inside-out membrane patches. Even in the presence of strong rectification, single-channel measurements could represent an even better approximation of undistorted conduction than could macroscopic currents. Current saturation at high  $K_{OUT}$  was observed by Sakmann and Trube (1984) in strong inward rectifier  $i_{K1}$  channels from guinea-pig hearts. Superficially, this is in contrast to our finding that at high  $[K_{OUT}]$  (and constant 150-mM  $[K_{IN}]$ ; positive  $E_K$ ) I-V relations are better described by the GHK equation than at low  $[K_{OUT}]$  (negative  $E_K$ ). However, even though I-V relations follow the GHK equation more closely at membrane potentials close to  $E_K$ , they are still linearized at more negative potentials. As Sakmann and Trube (1984) measured single-channel currents at  $-100$  mV, far negative to  $E_K$ , both I-V linearization and saturation of  $G_{REV}$  conductance would contribute to current saturation at high  $K_{OUT}$ .

Sakmann and Trube (1984) also showed that conductance of  $i_{K1}$  channels (mostly at low  $K_{OUT}$ ) is proportional to  $\sim K_{OUT}^{0.62}$ , which is close to the  $K_{OUT}$  dependence reported in other studies with native and cloned inward rectifier channels (Hagiwara and Takahashi, 1974; Kubo et al., 1993a; Perier et al., 1994; Makhina et al., 1994; Ho et al., 1993). However, it seems that this may not be a property that is unique to inward rectifier channels, because the simple GHK equation actually predicts that  $G \sim K_{OUT}^{0.5}$ . The present results indicate that this  $K_{OUT}$  dependence of conductance is a property of the open channel, as suggested by previous authors (Ciani et al., 1978; Sakmann and Trube, 1984).

Sakmann and Trube (1984) also noted that single-channel I-V relations for native cardiac inward rectifier  $i_{K1}$  channels are linearized at K<sup>+</sup> concentrations giving negative  $E_K$ . Other channels also display linearization of I-V curves (e.g., Chang et al., 1994; glutamate receptor channel). Some of the above results, for instance inward rectification in symmetrical solutions, might involve surface charge or related effects (Hille, 1992; Lu and Mackinnon, 1994b). Although these effects probably do play a role in ion conduction, especially over such wide ranges of [K<sup>+</sup>], they were not considered in the present modeling because the amount of available data is negligible compared with the flexibility of the model and it is apparent that the simple 2S3B model can predict properties such as inward rectification in symmetrical potassium, without involving additional effects (Hill and Chen, 1971).

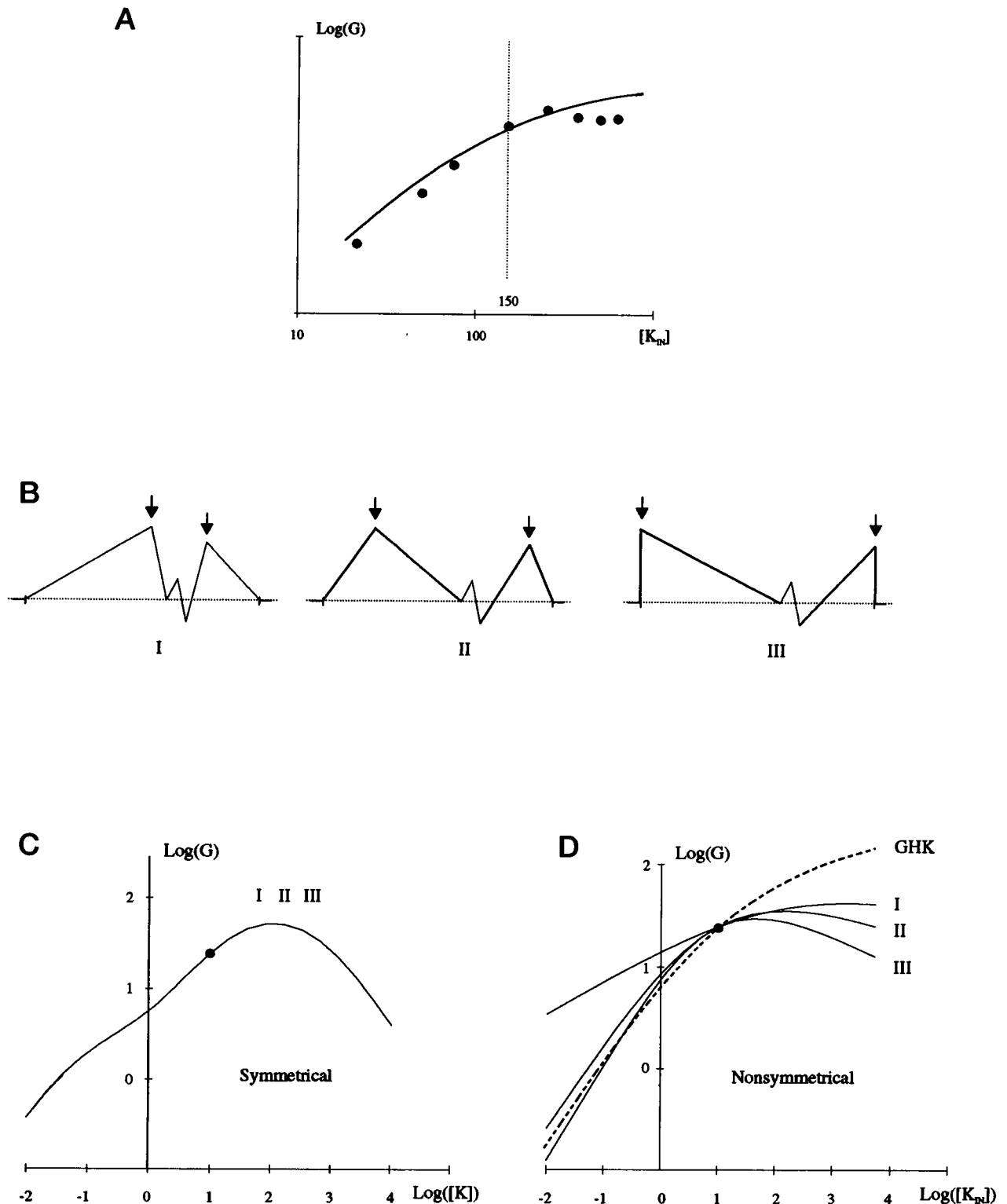


**FIGURE 7** Model dependence of conductance. (A) Experimental  $G_{REV}$  -  $[K_{IN}]$  relationship superimposed upon that predicted by the model in Fig. 6.  $K_{OUT}$  was kept at a control level corresponding to 150 mM ( $K_{IN}$  also in mM). (B) Three energy profiles differing in the positions of side peaks as indicated by the arrows. Model II corresponds to that in Fig. 6. (C) Conductance in the symmetrical K solutions does not depend on the position of the energy peaks (or of the energy wells, not shown). All three relations for energy profiles I-III coincide. (D) In nonsymmetrical solutions  $G_{REV}$  conductance "rectifies" more steeply when side energy peaks are located closer to the pore entrance. The dashed curve corresponds to  $G_{REV}$  derived from GHK equation (3).

The effects of internal [K<sup>+</sup>] on conductance of inward rectifier K channels have received less attention. Cohen et al. (1989) and Hagiwara and Yoshi (1979) observed a slight rightward shift in the midpoint of the conductance–voltage relationship when they lowered  $K_{IN}$  in cardiac Purkinje cells and starfish eggs, respectively. These results presumably reflect a small relief of the polyamine block as a result of lowering intracellular [K<sup>+</sup>]. However, the presence of polyamine-induced rectification in these studies obviates direct comparisons between them and the present results.

## CONCLUSIONS

After removal of inward rectification, we have examined the current through unblocked strong inward rectifier K channels (IRK1, Kir2.1). Unblocked IRK1 channel I–V relations show a mild inward rectification in symmetrical solutions and are linearized in nonsymmetrical solutions, particularly those that bring  $E_K$  to negative values. Channel conductance saturates when internal, or external, K concentration exceeds that on the other side of the membrane. As shown by others, with low  $K_{OUT}$ , or  $K_{IN}$ , conductance closely follows the predictions of the GHK equation, suggesting that the well-known “square-root” dependence of conductance of strong inward rectifiers on  $K_{OUT}$  reflects the properties of an unsaturated pore. A nonsymmetrical 2S3B model gives qualitatively good overall approximation for both I–V relations and the  $K_{IN}$  and  $K_{OUT}$  dependence of IRK1 conductance. Models with additional barriers would probably produce quantitative fits to the data.

Kir2.1 (IRK1) was a gift from Dr. Lou Philipson and Dr. Dottie Hanck (University of Chicago). This research was supported by grant HL54171 from the National Institutes of Health (to CGN) and an Established Investigatorship from the American Heart Association (to CGN).

## REFERENCES

- Alvarez, O., A. Villarroel, and G. Eisenman. 1992. Calculation of ion currents from energy profiles and energy profiles from ion currents in multibarrier, multisite, multioccupancy channel model. *Methods Enzym.* 207:816–854.
- Armstrong, C. M. 1969. Inactivation of the potassium conductance and related phenomena caused by quaternary ammonium ion injected in squid axons. *J. Gen. Physiol.* 54:553–575.
- Blatz, A. L., and K. L. Magleby. 1984. Ion conductance and selectivity of single calcium-activated potassium channels in cultured rat muscle. *J. Gen. Physiol.* 84:1–23.
- Cecchi, X., O. Alvarez, and D. Wolff. 1986. Characterization of a calcium-activated potassium channel from rabbit intestinal smooth muscle incorporated into planar bilayers. *J. Membr. Biol.* 91:11–18.
- Ciani, S., S. Krasner, S. Miyazaki, and S. Hagiwara. 1978. A model for anomalous rectification: electrochemical potential dependent gating of membrane channels. *J. Membr. Biol.* 44:103–134.
- Chang, H., S. Ciani, and Y. Kidokoro. 1994. Ion permeation properties of the glutamate receptor channel in cultured embryonic *Drosophila* myotubes. *J. Physiol.* 476:1–16.
- Chizmadjev, Yu. A., and S. Kh. Aityan. 1977. Ion transport across sodium channels in biological membranes. *J. Theor. Biol.* 64:429–453.
- Cohen, I. S., D. DiFrancesco, N. K. Mulrine, and P. Pennefather. 1989. Internal and external K<sup>+</sup> help gate the inward rectifier. *Biophys. J.* 55:197–202.
- Coronado, R., R. L. Rosenberg, and C. Miller. 1980. Ionic selectivity, saturation, and block in a K<sup>+</sup>-selective channel from sarcoplasmic reticulum. *J. Gen. Physiol.* 76:425–446.
- Eyring, H. 1935. The activated complex in chemical reactions. *J. Chem. Phys.* 3:107–115.
- Fakler, B., U. Brandle, C. Bond, E. Glowatzki, C. Konig, J. P. Adelman, H. P. Zenner, and J. P. Ruppersberg. 1994. A structural determinant of differential sensitivity of cloned inward rectifier K<sup>+</sup> channels to intracellular spermine. *FEBS Lett.* 356:199–203.
- Fakler, B., U. Brandle, E. Glowatzki, S. Weidemann, H. P. Zenner, and J. P. Ruppersberg. 1995. Strong voltage-dependent inward rectification of inward rectifier K<sup>+</sup> channels is caused by intracellular spermine. *Cell.* 80:149–154.
- Ficker, E., M. Taglialatela, B. A. Wible, C. M. Henley, and A. M. Brown. 1994. Spermine and spermidine as gating molecules for inward rectifier K<sup>+</sup> channels. *Science.* 266:1068–1072.
- Finkelstein, A., and O. S. Andersen. 1981. The gramicidin A channel: a review of its permeability characteristics with special reference to the single-file aspect of transport. *J. Membr. Biol.* 59:155–71.
- French, R. J., J. F. Worley 3rd, W. F. Wonderlin, A. S. Kularatna, and B. K. Krueger. 1994. Ion permeation, divalent ion block, and chemical modification of single sodium channels. Description by single- and double-occupancy rate-theory models. *J. Gen. Physiol.* 103:447–70.
- Goldman, D. E. 1943. Potential, impedance and rectification in membranes. *J. Gen. Physiol.* 27:37–60.
- Hagiwara, S., S. Miyazaki, S. Krasne, and S. Ciani. 1977. Anomalous permeabilities of the egg cell membrane of starfish egg cell. *J. Membr. Biol.* 18:61–80.
- Hagiwara, S., and K. Takahashi K. 1974. The anomalous rectification and cation selectivity of the membrane of a starfish egg cell. *J. Membrane Biol.* 18:61–80.
- Hagiwara, S., and M. Yoshii. 1979. Effects of internal potassium and sodium on the anomalous rectification of the starfish egg as examined by internal perfusion. *J. Physiol.* 292:251–265.
- Hill, T. L., and Y. Chen. 1971. Cooperative effects in models of steady-state transport across membranes. IV. One site, two-site, and multisite models. *Biophys. J.* 11:685–710.
- Hill, J. A., Jr., R. Coronado, and H. C. Strauss. 1989. Potassium channel of cardiac sarcoplasmic reticulum is a multi-ion channel. *Biophys. J.* 55:35–46.
- Hille, B. 1975. Ionic selectivity, saturation, and block in sodium channels. A four barrier model. *J. Gen. Physiol.* 66:535–560.
- Hille, B. 1992. *Ionic Channels of Excitable Membranes*. Sinauer Associates. Chap. 16.
- Hille, B., and W. Schwarz. 1978. Potassium channels as multi-ion single-file pores. *J. Gen. Physiol.* 72:409–442.
- Ho, K., C. G. Nichols, W. J. Lederer, J. Lytton, P. M. Vassilev, M. V. Kanazirska, and S. C. Hebert. 1993. Cloning and expression of an inwardly rectifying ATP-regulated potassium channel. *Nature (London).* 362:31–38.
- Hodgkin, A. L., and R. D. Keynes. 1955. The potassium permeability of a giant nerve fibre. *J. Physiol. (London)* 128:61–88.
- Katz, B. 1949. Les constantes electriques de la membrane du muscle. *Arch. Sci. Physiol.* 2:285–299.
- Kubo, Y., T. J. Baldwin, Y. N. Jan, and L. Y. Jan. 1993a. Primary structure and functional expression of a mouse inward rectifier potassium channel. *Nature (London).* 362:127–133.
- Kubo, Y., E. Reuveny, P. A. Slesinger, Y. N. Jan, and L. Y. Jan. 1993b. Primary structure and functional expression of a rat G-protein coupled muscarinic potassium channel. *Nature (London).* 364:802–806.
- Lopatin, A. N., E. N. Makhina, and C. G. Nichols. 1994. Potassium channel block by cytoplasmic polyamines as the mechanism of intrinsic rectification. *Nature (London).* 372:366–369.
- Lopatin, A. N., E. N. Makhina, and C. G. Nichols. 1995. The mechanism of inward rectification of potassium channels. *J. Gen. Physiol.* 106:923–955.

- Lu, Z., and R. MacKinnon. 1994a. A conductance maximum observed in an inward rectifier potassium channel. *J. Gen. Physiol.* 104:477–486.
- Lu, Z., and R. MacKinnon. 1994b. Electrostatic tuning of  $Mg^{2+}$  affinity in an inward rectifier  $K^+$  channel. *Nature (London)*. 371:243–246.
- Makhina, E. N., A. J. Kelly, A. N. Lopatin, R. W. Mercer, and C. G. Nichols. 1994. Cloning and expression of a novel inward rectifier potassium channel from human brain. *J. Biol. Chem.* 269:20468–20474.
- Matsuda, H., A. Saigusa, and H. Irisawa. 1987. Ohmic conductance through the inwardly rectifying  $K^+$  channel and blocking by internal  $Mg^{2+}$ . *Nature (London)*. 325:156–159.
- Neyton, J., and C. Miller. 1988. Potassium blocks barium permeation through a calcium-activated potassium channel. *J. Gen. Physiol.* 92:549–567.
- Nichols, C. G. 1993. The “inner core” of inward rectifier potassium channels. *Trends Pharmacol. Sci.* 14:320–323.
- Perier, F., C. M. Radeke, and C. A. Vandenberg. 1994. Primary structure and characterization of a small-conductance inwardly rectifying potassium channel from human hippocampus. *Proc. Natl. Acad. Sci. USA*. 91:6240–6244.
- Sakmann, B., and G. Trube. 1984. Conductance properties of single inwardly rectifying potassium channels in ventricular cells from guinea-pig heart. *J. Physiol.* 347:641–657.
- Schumaker, M. F., and R. MacKinnon. 1990. A simple model for multi-ion permeation. Single vacancy conduction in a simple pore model. *Biophys. J.* 58:975–984.
- Shapiro, M. S., and T. E. DeCoursey. 1991. Selectivity and gating of the type L potassium channel in mouse lymphocytes. *J. Gen. Physiol.* 97:1227–1250.
- Tang, J. M., J. Wang, and R. S. Eisenberg. 1992. Perfusing patch pipettes. *Methods Enzymol.* 207:176–81.
- Vandenberg, C. A. 1987. Inward rectification of a potassium channel in cardiac ventricular cells depends on internal magnesium ions. *Proc. Nat. Acad. Sci. USA*. 84:2560–2562.
- Villarroel, A., O. Alvarez, and G. Eisenman. 1988. A maximum in conductance occurs for the large  $Ca^{2+}$ -activated  $K^+$  channel at high  $Rb^+$  concentration. *Biophys. J.* 53:259a.
- Wagoner, P. K., and G. S. Oxford. 1987. Cation permeation through the voltage-dependent potassium channel in the squid axon. Characteristics and mechanisms. *J. Gen. Physiol.* 90:261–290.
- Yang, J., Y. N. Jan, and L. Y. Jan. 1995. Control of rectification and permeation by residues in two distinct domains in an inward rectifier  $K^+$  channel. *Neurone*. 14:1047–1054.